

Isoform specific phosphorylation of p53 by protein kinase CK1

Andrea Venerando · Oriano Marin ·
Giorgio Cozza · Victor H. Bustos · Stefania Sarno ·
Lorenzo Alberto Pinna

Received: 31 July 2009 / Revised: 18 November 2009 / Accepted: 14 December 2009 / Published online: 30 December 2009
© Birkhäuser Verlag, Basel/Switzerland 2009

Abstract The ability of three isoforms of protein kinase CK1 (α , γ_1 , and δ) to phosphorylate the N-terminal region of p53 has been assessed using either recombinant p53 or a synthetic peptide reproducing its 1–28 sequence. Both substrates are readily phosphorylated by CK1 δ and CK1 α , but not by the γ isoform. Affinity of full size p53 for CK1 is 3 orders of magnitude higher than that of its N-terminal peptide (K_m 0.82 μ M vs 1.51 mM). The preferred target is S20, whose phosphorylation critically relies on E17, while S6 is unaffected despite displaying the same consensus (E-x-x-S). Our data support the concept that non-primed phosphorylation of p53 by CK1 is an isoform-specific reaction preferentially affecting S20 by a mechanism which is grounded both on a local consensus and on a remote docking site mapped to the K²²¹RQK²²⁴ loop according to modeling and mutational analysis.

Keywords Casein kinase 1 · CK1 · CKI · p53 phosphorylation · p53 Ser20

Introduction

The acronym CK1 (derived from the misnomer, casein kinase 1) denotes a small independent sub-family of the kinome composed in mammalian of seven kinases, CK1 α , β , γ_1 , γ_2 , γ_3 , δ , and ϵ . Given the very high similarity among the three γ isoforms and between α and δ/ϵ , CK1 isoforms can be grouped into three main classes: α , γ , and δ [1]. While the crystal structure of enzymes belonging to the δ (PDB code: 1CKI; 1CSN) and γ (PDB code: 2CMW; 2C47; 2CHL) isoforms have been solved [2, 3], structural information of CK1 α is not yet available.

Taken collectively, CK1 enzymes have been implicated in a variety of biological functions, including chromosome segregation [4, 5], spindle formation [6–8], circadian rhythm [9], nuclear import [10], Wnt pathway [11–17], and apoptosis [18, 19]. Deregulation of CK1 isoforms has been described in neurodegenerative and sleeping disorders [20–22], and in cancer [23–26]. Recently, silencing of CK1 has been associated with the disappearance of metastases formation [27].

Features underlying substrate specificity by CK1 are still a matter of debate and investigation, a circumstance which makes it difficult to predict residues phosphorylated by CK1 in its potential substrates and to evaluate the actual contribution of CK1 to available phosphoproteome data bases. Early studies mostly performed with artificial substrates revealed that CK1 is a “phosphate directed” protein kinase, able to phosphorylate with high efficiency Ser/Thr residues specified by a pre-phosphorylated side chain (either pS or pT) at position n-3 [28–30], which could not be efficiently replaced by the negatively charged side chains of glutamic and aspartic acid. This led to the concept of “hierarchical phosphorylation” [31] and to the definition of “primed” or “priming” to indicate kinases

A. Venerando · O. Marin · V. H. Bustos · S. Sarno · L. A. Pinna
Venetian Institute of Molecular Medicine (VIMM),
Via G. Orus, 2, 35129 Padova, Italy

A. Venerando · O. Marin · G. Cozza · S. Sarno ·
L. A. Pinna (✉)
Department of Biological Chemistry, University of Padova,
Viale G. Colombo, 3, 35131 Padova, Italy
e-mail: lorenzo.pinna@unipd.it

Present Address:

V. H. Bustos
Laboratory of Molecular and Cellular Neuroscience,
The Rockefeller University, New York, NY 10065, USA

which either need a phosphate in their consensus sequence or generate consensus sequences for other kinases by phosphorylating residues at given positions, respectively. In this respect, it soon became clear that CK1 is not necessarily a primed kinase, as many of its physiological substrates do not contain phosphorylated residues, while it often acts as a priming kinase, as its intervention is required to generate the consensus sequence for phosphate-directed kinases, with special reference to GSK3 [32–36]. Looking at the growing list of non-primed CK1 sites, it appears that only a few (e.g., the one in DARP-P32 [37]) are specified by clusters of acidic residues shown to be able to effectively replace the individual phosphorylated determinant at position n-3 [38], while the majority are to be considered as non-canonical sites whose targeting by CK1 depends on different and somewhat variable local determinants [39–41]. While these atypical local determinants also appear to be important for the phosphorylation of the full-length protein substrate, they are not sufficient alone to confer high affinity for the kinase, as revealed by high K_m values of the peptide substrates (close to the millimolar range) as compared to those calculated with the whole protein. In the case of β -catenin, we have shown that the difference is accounted for by a remote docking site located in the first Armadillo repeat of β -catenin whose removal causes a 3 orders of magnitude rise in the K_m value [41].

Among well-established non-primed substrates of CK1, p53 deserves special attention due to the fundamental and complex role of this multiphosphorylated tumor suppressor protein. Not less than 17 phosphorylated residues have been detected in human p53 [42], whose phosphorylation is promoted by a variety of protein kinases each of which in turn may impinge on more than one residue. Many of these residues are clustered in the N-terminal region, whose phosphorylation is generally believed to increase the level and stability of p53 by reducing the interaction with the main negative regulator MDM2 while promoting the binding of the acetyltransferase P300 [43]. These are seryl residues 6, 9, 15, 20, 33, 37, and 46 and the threonyl residue 18 [44]. They share the property of being phosphorylated in response to ionizing radiations or UV light, but a complex panel of partially unidentified protein kinases are responsible for their individual phosphorylation. In particular, CK1 has been implicated in the phosphorylation of S6 and S9 (in a hierarchical fashion) [45–47] and of T18 [48, 49], an event primed by previous phosphorylation of S15 by a variety of kinases, including DNA-PK [50], ATM [51], ATR [52], ERKs, and p38 [53]. Recently, however, the characterization of a kinase responsible for the phosphorylation of p53 at S20 in response to DNA viral infections led to its identification as CK1 α [54]. This came as a surprise, since S20 was previously reported to be a target of kinases other than CK1,

notably CHK1/CHK2 [55, 56], JNK, and MAPKAPK2 [57]. In order to shed light on the actual aptitude of different CK1 isoforms to phosphorylate individual residues in the N-terminus of p53, we have undertaken an investigation exploiting three purified recombinant isoforms of CK1, α , γ_1 , and δ , this latter either full length or with a C-terminal truncation making it substantially identical to the corresponding truncated form of CK1 ϵ . These were tested for their aptitude to phosphorylate either a set of synthetic peptides encompassing with suitable substitutions the 1–28 N-terminal segment of p53 or recombinant p53 (residues 1–363) expressed in bacteria, in order to avoid post-translational modification which would hinder the interpretation of our results and prevent any reliable kinetic comparison with the corresponding peptides. The data presented show that, while p53 displays for CK1 a 3 orders of magnitude higher affinity than its N-terminal segment (as judged from K_m values), it shares with it a special susceptibility to the δ isoform which preferentially phosphorylates S20 in both the protein and the peptide. Conversely, primed phosphorylation of T18 in a peptide chemically phosphorylated at S15 is readily performed with comparable efficiencies by any of the α , the γ_1 , or the δ isoforms of CK1.

Materials and methods

Materials

Solvents and coupling reagents for peptide synthesis were from Applied Biosystems (Foster City, CA). Protected amino acids were from Novabiochem (brand of Merck, Darmstadt, Germany). All other analytical grade reagents were from Sigma–Aldrich (St. Louis, MO). Monoclonal antibody against p53 and phospho-p53 (Ser6), (Ser9), (Ser15), (Thr18), (Ser20), (Ser37), (Ser46), (Ser392) antibodies were from Cell Signaling Technology (Beverly, MA). [γ - ^{33}P]ATP (3,000 Ci/mmol) was purchased from Perkin Elmer (Waltham, MA). Plasmid pGEX-4T1 for GST-hp53 was kindly supplied by Dr. Michelangelo Cordenonsi (Padua).

Synthetic peptides

The p53-derived synthetic peptides on display in Table 1 were synthesized by solid phase peptide synthesis method using a multiple peptide synthesizer SyroII (MultiSynTech, Witten, Germany) on 4-Hydroxymethylphenoxyacetyl PEGA resin (Novabiochem) solid support. The 9-fluorenylmethoxycarbonyl (Fmoc) strategy [58] was applied throughout the peptide chain assembly, using 2-(1H-benzotriazol-1-yl)-1,1,3,3-tetramethyluronium hexafluorophosphate (HBTU) and

Table 1 N-terminal p53 peptides used in the present study

The wild-type peptide reproduces the 1–28 sequence of human p53 with the addition of two C-terminal lysine residues (in italics) required for protein kinase assay by phosphocellulose p81 paper absorption method. Residues substituted relative to wild-type are in bold. For details, see “Materials and methods”

pS Phosphoserine

| Conventional name | Amino acids sequence |
|-------------------|---|
| WT | MEEPQSDPSVEPPLSQETFSDLWKLLPEKK |
| S6A | MEEPQADPSVEPPLSQETFSDLWKLLPEKK |
| S9A | MEEPQSDPAVEPPLSQETFSDLWKLLPEKK |
| S15A | MEEPQSDPSVEPPLAQETFSDLWKLLPEKK |
| E17A | MEEPQSDPSVEPPLSQATFSDLWKLLPEKK |
| S20A | MEEPQSDPSVEPPLSQETFADLWKLLPEKK |
| S6S9AA | MEEPQADPAVEPPLSQETFSDLWKLLPEKK |
| S15S20AA | MEEPQSDPSVEPPLAQETFADLWKLLPEKK |
| S6S9S15AAA | MEEPQADPAVEPPLAQETFSDLWKLLPEKK |
| S6S9S20AAA | MEEPQADPAVEPPLSQETFADLWKLLPEKK |
| S6S9S15E17AAAA | MEEPQADPAVEPPLAQATFSDLWKLLPEKK |
| pS6S15S20AA | MEEPQ p SDPSVEPPLAQETFADLWKLLPEKK |
| pS15 | MEEPQSDPSVEPPL p SQETFSDLWKLLPEKK |
| pS20 | MEEPQSDPSVEPPLSQET p SDLWKLLPEKK |
| pS6pS9 | MEEPQ p SD p SVEPPLSQETFSDLWKLLPEKK |
| pS6pS9pS15 | MEEPQ p SD p SVEPPL p SQETFSDLWKLLPEKK |

1-hydroxybenzotriazole (HOBt) as coupling reagents. The side-chain protected amino acid building blocks were as follows: Fmoc-Glu(tert-butyl), Fmoc-Asp(tert-butyl), Fmoc-Ser(tert-butyl), Fmoc-Ser(PO(Bzl)OH), Fmoc-Thr(tert-butyl), Fmoc-Lys(tert-butyloxycarbonyl), Fmoc-His(trityl), Fmoc-Gln(trityl), and Fmoc-Trp(tert-butyloxycarbonyl). Cleavage of the peptides was performed by reacting the peptidyl-resins with a mixture containing trifluoroacetic acid/water/thioanisole/ethanedithiol/phenol (10 ml/0.5 ml/0.5 ml/0.25 ml/750 mg) for 2.5 h. Crude peptides were purified by a preparative reverse phase HPLC. Molecular masses of the peptides were confirmed by mass spectroscopy on a model 4800 MALDI TOF-TOF mass spectrometer (Applied Biosystems). The purity of the peptides was in the range 95–98% as evaluated by analytical reverse phase HPLC. Additionally, two lysine residues were introduced at C-terminal side of each peptide. Such a basic motif was essential for the protein kinase assay based on phosphocellulose paper substrate absorption.

Protein cloning, expression, and purification

The clones of CK1 α (gene code Q8JGT0) and CK1 δ (isoform B, gene code Q6P3K7) from zebrafish (*Danio rerio*), and the clone of CK1 γ_1 (gene code Q5PRD4) from rat were obtained as described previously [36, 59]. All the isoforms of CK1 contained six histidines in the N-terminus to facilitate the purification. The delta isoform was obtained either full length or with a C-terminal truncation (Δ 317). This latter, which is nearly indistinguishable from the corresponding sequence of the ϵ isoform (95% identity), was used throughout the paper, unless indicated

differently. Two mutants of CK1 $\delta^{\Delta 317}$ (K221L and K224A) were generated with the QuikChange Site-Directed Mutagenesis Kit (Stratagene, La Jolla, CA) using the forward and reverse primer oligonucleotides as follows: for K221L, 5'-GAAAGCCGCCACCTTGAGACAGAAGTATGAGCG-3' and 5'-CGCTCATACTTCTGTCTCAAGGTGCGGCTTTC-3', respectively; for K224A, 5'-GCCGCCACCAAGAGACAGGCGTATGAGCGTATC-3' and 5'-GATACGCTCATACGCCTGTCTCTTGGTGGCGGC-3', respectively. The E17A p53 mutant was generated with the QuikChange Site-Directed Mutagenesis Kit using pGEX-4T1-hp53 as template and forward and reverse primer oligonucleotides as follows: 5'-CCTCTGAGTCAGGCAACATTTTCAGACC-3' and 5'-GGTCTGAAAATGTTGCC TGACTCAGAGG-3', respectively. The mutations were confirmed by DNA sequencing.

Protein expression and purification

CK1 α and CK1 γ were expressed in *Escherichia coli* BL21(DE3) cells. The plasmids of CK1 δ (full length, Δ 317 and its mutants) were used to transform *E. coli* strain B834. Cells were grown at 37°C to an OD₆₀₀ of 0.5–0.6. At this point, protein expression was induced by adding isopropyl β -D-thiogalactoside (IPTG) to a final concentration of 0.3, 0.8, and 1 mM for CK1 α , CK1 γ , and CK1 δ , respectively. Induction was carried out overnight at 20°C in the case of CK1 α and CK1 δ , while for CK1 γ , the temperature was 25°C. Afterwards, the cells were harvested by centrifugation at 3,000g for 20 min at 4°C, and resuspended in lysis buffer (50 mM Tris/HCl, pH 8.0, 20% v/v glycerol, and 0.5 M NaCl, supplemented with protease inhibitor cocktail from Sigma). Cells were lysed by French press. The

soluble fraction, obtained after 30 min of centrifugation at 10,000g, was applied onto Ni-NTA-agarose columns (Sigma) equilibrated with the lysis buffer. The columns were extensively washed and the proteins were subsequently eluted with a buffer containing 50 mM Tris/HCl, pH 6.8, 5% v/v glycerol, 50 mM NaCl, and 300 mM imidazole. CK1 γ and CK1 δ were further purified by gel filtration with Superdex 75 10/300GL column (Amersham Pharmacia Biotech) equilibrated in a buffer containing 25 mM Tris/HCl, pH 7.0, 0.1 M NaCl, and 1 mM dithiothreitol (DTT).

GST-fusion protein of human recombinant p53 and its E17A mutant were expressed in *E. coli* BL21(DE3) cells. Cells were grown at 37°C to an OD₆₀₀ of 0.7. Protein expression was induced by adding 1 mM IPTG and it was allowed to proceed for 4 h at 30°C. Afterward, cells were pelleted at 3,000g for 20 min at 4°C, and cell pellets were resuspended in PBS, added with protease inhibitors, and lysed using a French press. After centrifugation at 10,000g for 30 min, the supernatant was loaded onto Glutathione-Sephrose 4 Fast Flow columns (GE-Healthcare, UK), equilibrated with binding buffer (PBS, pH 7.3, and 1 mM DTT). Proteins were eluted with a buffer containing 50 mM Tris/HCl, 0.1 M NaCl, 1 mM DTT, and 10 mM glutathione, and the most pure fractions were pooled, concentrated, and applied onto a gel filtration Superdex 200 HiLoad 26/60 column (Amersham Pharmacia Biotech), equilibrated in a buffer containing 25 mM Tris/HCl, pH 8, 0.1 M NaCl, 10% v/v glycerol, and 1 mM DTT. Untagged recombinant p53 was obtained by cleaving GST-p53 bound to the Glutathione-Sephrose 4 Fast Flow resin (GE-Healthcare) in the presence of 40 U of thrombin at 4°C over night. The column was washed with 50 mM Tris/HCl, 0.1 M NaCl, 10% v/v glycerol, and 1 mM DTT; the fractions containing untagged p53 were collected, concentrated, and applied onto a gel filtration Superdex 200 HiLoad 26/60 column (Amersham Pharmacia Biotech) for a further purification. Its apparent MW, as assessed by gel filtration experiments, was consistent with a tetrameric form of p53.

Phosphorylation assays

Reaction conditions for peptide phosphorylation experiments were the following: a range of concentration of synthetic peptides derived from human p53 N-terminal region were phosphorylated by incubation in a 20- μ l volume containing 50 mM Tris/HCl, pH 7.5, 10 mM MgCl₂, 100 mM NaCl, and 50 μ M [γ -³³P]ATP (specific radioactivity 1,500–2,000 cpm/pmol). The reaction was started by the addition of protein kinases CK1 α , CK1 γ , and CK1 δ (either full length or Δ 317) normalized against a common peptide substrate, derived from Inhibitor-2 of protein phosphatase-1 (the “I-2” peptide RRRKHAIGDDDDAY

SITA) [60], as previously described [36]. More precisely, each amount of CK1 isoform displayed with I-2 peptide an activity of 12 pmol of phosphate transferred per minute. The reaction mixtures were incubated for the indicated time at 37°C and stopped by ice cooling and absorption on phospho-cellulose p81 paper. Papers were washed three times with 75 mM phosphoric acid, dried, and counted in a scintillation counter. Reaction conditions for full-length p53 phosphorylation were identical to those used for peptide phosphorylation except for the replacement of the peptide with full-length p53, either GST-tagged or deprived of the tag at concentrations ranging between 30 nM and 2.5 μ M. The reaction was stopped by the addition of 5 \times concentrated Laemmli buffer and boiling followed by SDS-polyacrylamide gel electrophoresis (SDS-PAGE), Coomassie staining, and autoradiography (PerkinElmer's Cyclone Plus Storage Phosphor System). Results are representative of at least three independent experiments. ³³P incorporation was evaluated by excision of protein bands from the gel followed by counting in a scintillation counter.

Initial rate data were fitted to the Michaelis–Menten equation with the program Prism (GraphPad Software, La Jolla, CA) to obtain K_m and V_{max} values.

Phospho-aminoacids analysis

After phosphoradiolabeling, peptides were separated from reaction mixture by filtration on Strata C18-E columns (Phenomenex, Torrance, CA), lyophilized, and digested with 6 N HCl for 4 h at 110°C. Each sample was subjected to high-voltage paper electrophoresis at pH 1.9 for 2.5 h, in the presence of non-radioactive phospho-amino acids, as migration reference, followed by autoradiography [61].

Western blotting

GST-p53 proteins after in vitro kinase reaction were resolved by 11% SDS-PAGE, and transferred onto Immobilon-P membranes (Millipore, Billerica, MA). Membranes were probed with the indicated antibody, and detected by ECL (enhanced chemiluminescence; Amersham Biosciences). Quantitation of the signal was obtained by chemiluminescence detection on Kodak Image Station 440cf (Eastman Kodak, New Haven, CT) and by analysis with the Kodak 1D image software.

Protein–protein docking

For the computer-aided protein–protein docking stages, rat CK1 δ isoform and the mouse p53 were retrieved from the PDB (PDB code: 1CKJ and 2IOI, respectively). Hydrogen atoms were added to the protein structure using standard

geometries with the MOE program [62]. To minimize contacts between hydrogens, the structures were subjected to Amber99 force field minimization until the rms of conjugate gradient was $<0.1 \text{ kcal mol}^{-1} \text{ \AA}^{-1}$, keeping the heavy atoms fixed at their crystallographic positions [62]. After this initial in silico approach, a set of protein–protein docking experiments was performed. Protein–protein docking is a computational tool useful for predicting the 3D structure of protein complexes from the coordinates of its subunits. We have adopted a two-stage approach, which recently proved quite successful [63, 64]; in the first stage, the two monomers were treated as rigid bodies and all the rotational and translational degrees of freedom were fully explored, using a cluster of protein–protein docking algorithms (Zdock, Gramm and Echer); in the second stage, a small number of structures deriving from the initial stage was refined in the docking zone using side-chain rotamers and energy-minimization strategy.

Results

Several phosphorylated residues, generated by the concerted action of a variety of protein kinases, are clustered in the N-terminal segment of p53 [42]. These include the aminoacids phosphorylated by CK1, whose precise identification is still a matter of debate. A priori, the only residues displaying a canonical sequence (E/D-x-x-S) for non-primed phosphorylation by CK1 appear to be S6, (which, once phosphorylated, could prime subsequent phosphorylation of S9) and S20. In turn, S15, believed to be a substrate of kinases other than CK1 (DNA-PK [50], ATM [51], ATR [52], ERKs, and p38 [53]), once phosphorylated is in the right position to prime phosphorylation of T18 by CK1 [48, 49]. Given these premises, peptides encompassing the N-terminal segment of p53 have been widely employed in mechanistic studies dealing with the implication of CK1 (and also of other kinases) in p53 phosphorylation [44, 45, 48].

We therefore started our investigation by assaying a peptide encompassing residues 1–28 of p53 for its ability to undergo phosphorylation by different isoforms of CK1, namely the α , γ , and δ isoforms. The peptide concentration was 1 mM and equi-active amounts of the CK1 isoforms were used, normalized for displaying identical activity toward a common peptide substrate (see “Materials and methods”). Under these comparable conditions, the time courses of phosphorylation reported in Fig. 1 were obtained: they show that, while the peptide is readily phosphorylated by CK1 δ , phosphorylation by CK1 α was much less pronounced, and that by the γ isoform was hardly detectable. Note that phosphorylation by C-terminally deleted CK1 δ isoform, which is substantially identical to

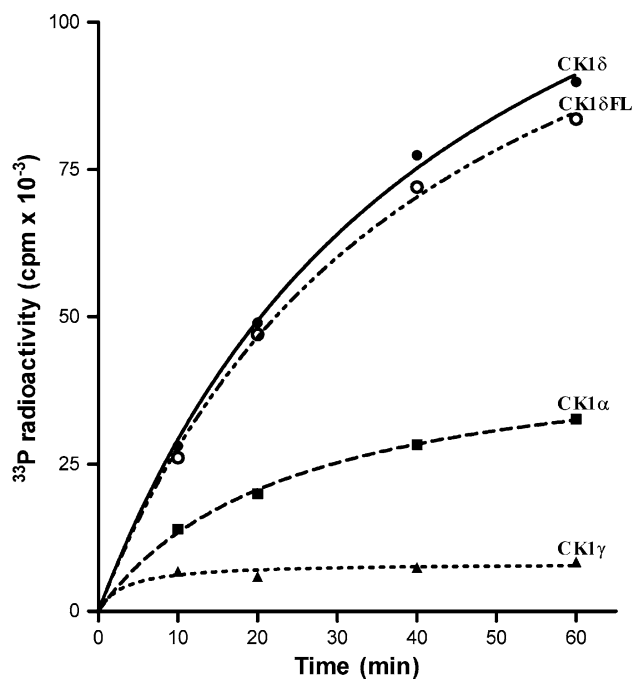


Fig. 1 Time-courses of phosphorylation of p53_[1–28] peptide by CK1 isoforms. Phosphorylation was performed in the presence of equi-active amounts of the indicated CK1 isoforms, as detailed in “Materials and methods”. The peptide concentration was 1 mM

CK1 ϵ (see “Materials and methods”) is superimposable on that of full-length CK1 δ . Phospho-aminoacid analysis revealed only phospho-serine, ruling out any appreciable phosphorylation of T18 (Fig. 2, lane 1).

To gain information about the seryl residues phosphorylated in the p53 peptide, these were individually or multiply replaced by the non-phosphorylatable residue alanine (see Table 1). The phosphorylation rates of the substituted peptides relative to the parent peptide (wild-type) are shown in Fig. 3a. While substitution of S6 and S9 (either single or double) reduces phosphorylation by less than 30%, a much more dramatic drop in phosphorylation rate was observed upon substitution of both seryl residues 15 and 20, consistent with the view that S15 and/or S20 are the main target(s) of CK1 δ . The actual implication of S20 rather than S15 is supported by the additional finding that replacement of S20 with alanine is detrimental both in the wild-type peptide and in the S6S9-substituted one. By sharp contrast, the individual replacement of S15 did not decrease but slightly increases the phosphorylation rate of the wild-type peptide. The same phosphorylation patterns were obtained by replacing truncated CK1 δ with either full-length CK1 δ or CK1 α (data not shown).

These data are consistent with the conclusion that the main CK1 δ and CK1 α target in the N-terminal segment of p53 is S20 whose replacement with alanine is invariably causative of a dramatic drop in phosphorylation rate

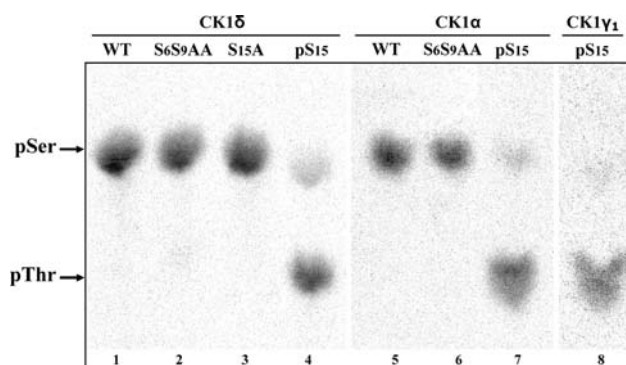


Fig. 2 Phosphoamino acid analysis of high-voltage paper electrophoresis. Peptides (0.5 mM) were incubated with indicated CK1 isoforms for 60 min in the presence of radioactive phosphorylation mixture. ^{33}P -radiolabeled peptides (as indicated) were hydrolyzed in 6 N HCl at 110°C for 4 h, and subjected to high-voltage paper electrophoresis followed by autoradiography for the identification of the phospho-amino acid (see “Materials and methods”). The position of phospho-amino acids (pSer and pThr), determined by cold standard migration, is indicated by the arrows

whether it is performed in the wild-type or in the S15A or in the S6S9AA peptides (85, 80, and 94%, respectively). Interestingly, S20 phosphorylation by CK1 is clearly relying on the weak consensus generated by a glutamic acid at position n-3 (E-t-f-S²⁰), as the replacement of this residue (E17) with alanine, either in the wild-type peptide or in the triply substituted one (S6S9S15AAA) has a detrimental effect, comparable to that of the replacement of S20 itself (see Fig. 3a). Minor phosphorylation of S6 and/or S9, on the other hand, is consistent with residual (around 20%) phosphorylation of the S15S20-substituted peptide and with decreased phosphorylation observed by replacing serines 6 and 9 in the wild-type peptide (about 25%) and, even more in the S15A-substituted peptide. Of note in this respect is the significant drop in phosphorylation rate promoted by the S9 substitution as opposed to the almost negligible effect of the S6 substitution. These data suggest that a significant albeit weak non-primed phosphorylation of S9, but not of S6, is catalyzed by CK1 δ and CK1 α . Non-primed phosphorylation of T18 has to be ruled out in any case since no detectable phospho-threonine could be isolated from the wild-type or S15A or S6S9AA peptides ^{33}P -radiolabeled by either CK1 δ or CK1 α (see Fig. 2, lanes 1–3 and 5–6, respectively).

It is worth noting in this respect that if S15 instead of being replaced by alanine is substituted by a phosphoserine, thus mimicking a reaction occurring in vivo by the intervention of various protein kinases, notably DNA-PK [50], the radioactivity incorporated by CK1 δ is dramatically increased (see Fig. 3b) being now almost entirely accounted for by phospho-threonine (Fig. 2, lane 4). This leads to the conclusion that, while S20 is the main non-primed target of CK1 δ , preferentially affected when the pS3 peptide is not

phosphorylated, once S15 is phosphorylated, primed phosphorylation of T18 becomes predominant over non-primed phosphorylation of S20. It is also worth noting in this respect that, while non-primed phosphorylation of S20 is catalyzed by the δ and to a lesser extent by the α isoform but not by the γ_1 isoform (see Fig. 1), primed phosphorylation of T18 in the pS15 peptide can also be performed by all three γ isoforms of CK1 (Fig. 3b–d), though in the case of CK1 γ_1 , it is still much less pronounced than that mediated by CK1 δ . The possibility that variable phosphorylation of the pS15 peptide by CK1 isoforms could be due to the targeting of different residues was ruled out by showing that T18 was the main phospho-acceptor residue, regardless to the isoform used (see Fig. 2, lanes 4, 7, 8). The priming potential of S6 appears to be weaker than that of S15 since its chemical phosphorylation within a peptide, in which S15 and S20 have been replaced by alanine, promotes a moderate phosphorylation of S9 by CK1 δ and α , having no effect at all with CK1 γ_1 (see Fig. 3, compare panels b, c, d). We have also examined the behavior of additional phosphopeptides, singly phosphorylated on S20, or doubly phosphorylated on S6 and S9, or triply phosphorylated on S6, S9, and S15. Their phosphorylation by CK1 δ is shown in Fig. 3b. Previous phosphorylation of S20 has a detrimental effect comparable to its replacement with alanine, reinforcing the conclusion that S20 is the main target of CK1 which becomes nearly inactive whenever S20 is no longer available as a phosphoacceptor residue. Quite unexpectedly, the doubly phosphorylated peptide pS6pS9 has lost any susceptibility to CK1 catalyzed phosphorylation. This is probably an artefact due to cyclization of the phosphopeptide through electrostatic interaction between the phosphates and the two C-terminal lysines added for rendering possible the phosphorylation assay with phosphocellulose paper (see Table 1). This point of view, supported by dynamic modelization (not shown), is also corroborated by the triply phosphorylated peptide (pS6, pS9, pS15) where primed phosphorylation of T18 becomes eightfold slower than that of its congener singly phosphorylated at S15 (Fig. 3b).

From the kinetic constants presented in Fig. 4, it appears that the p53 N-terminal peptides display with either the δ or the α isoforms K_m values around 1 mM, denoting low affinity for CK1. This also seems to be a common feature of peptides reproducing phosphoacceptor sites for CK1 in other physiological substrates, notably NF-AT4, β -catenin and APC [36, 39, 41]. Interestingly, it has been shown that such a weakness of the local determinants may be compensated for by remote docking sites which in the case of β -catenin cause a drop in K_m value from over 1 mM to 0.19 μM [41].

We therefore suspected that a similar situation may also apply to p53, and to assess this point we have run kinetics with full length p53 replaced for the p53_[1–28] peptide.

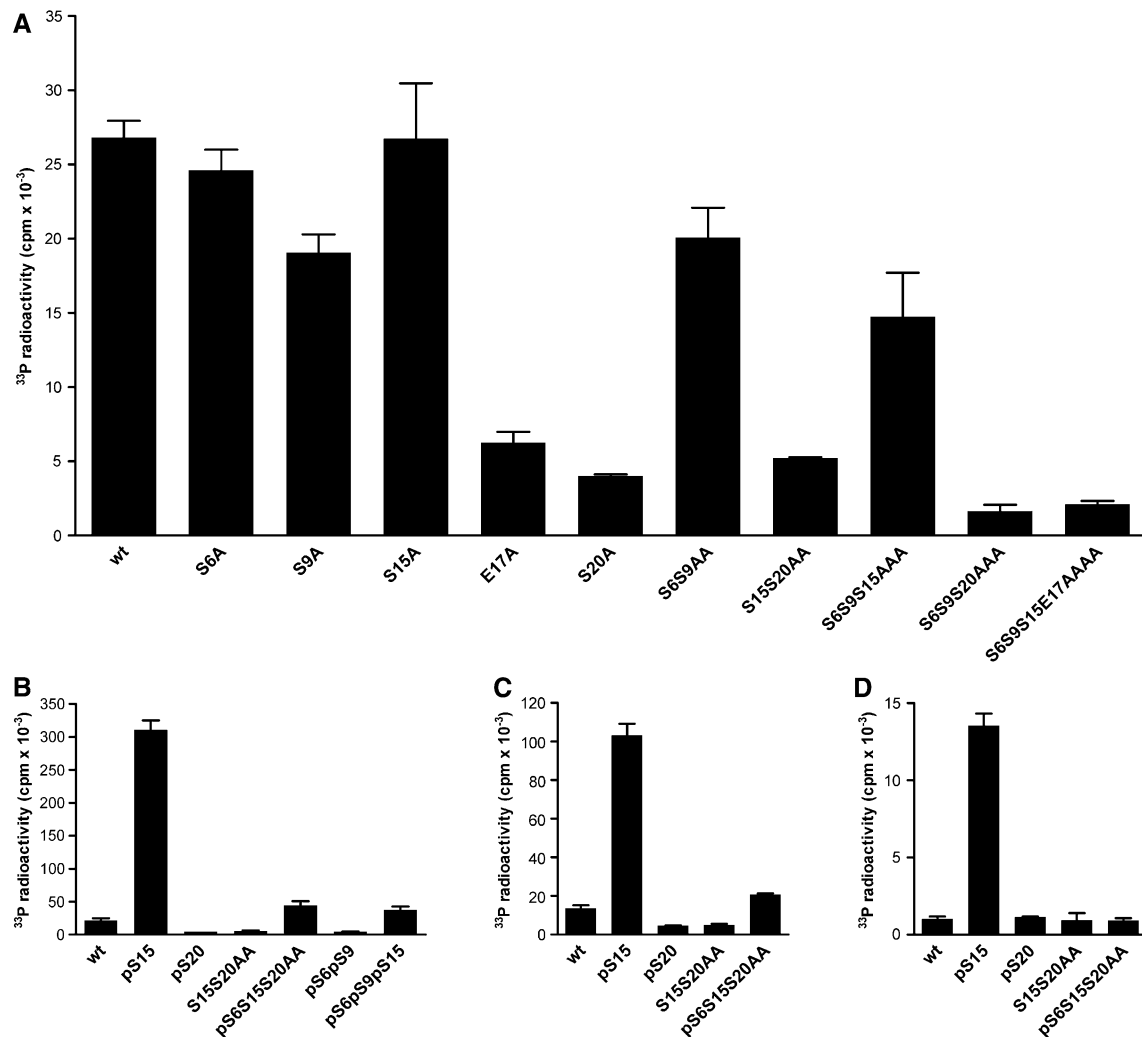


Fig. 3 Phosphorylation of substituted p53 N-terminal peptides by CK1. **a** The effect due to replacing serines and E17 with alanine is analyzed. Phosphorylation was performed by incubation with CK1 δ for 10 min at 37°C. A superimposable histogram was obtained by replacing CK1 δ with CK1 α . **b–d** p53 phosphopeptides (as indicated)

underwent phosphorylation assays in the presence of CK1 δ , CK1 α , and CK1 γ 1, respectively. Phosphorylation rates of the unprimed peptides, WT and S15S20AA, is also reported for comparison. For peptide nomenclature, see Table 1. The concentration of the peptides was 1 mM

The phosphorylating enzyme was CK1, either α , or γ 1, or δ isoforms. As in the case of the p53 peptide, the γ isoform proved unable to catalyze any significant phosphorylation of full-length p53; the α isoform, however, albeit less active than δ on the peptide (see Fig. 1), was able to phosphorylate full-size p53 with kinetics comparable to those of the δ isoform (Fig. 5a). Note that with both isoforms the K_m is in the submicromolar range, highlighting a 3 orders of magnitude higher affinity of CK1 δ and CK1 α for the full size protein as compared to the derived peptide. By sharp contrast the V_{max} with the peptide is about 50-fold higher than with the full-size protein as also observed with other CK1 substrates [40, 41]. We can conclude therefore that unprimed full-length p53 can be efficiently phosphorylated by both the α and δ but not by the γ isoform of CK1. Also noteworthy are the identical kinetic constants

calculated using either full length or truncated CK1 δ . This latter displays a nearly 100% identity with the corresponding sequence of the ϵ isoform, consistent with the knowledge that p53 is also readily phosphorylated by CK1 ϵ [7, 45].

To localize the residues affected by CK1 in full-length p53, advantage has been taken of commercially available phosphospecific antibodies raised against individual p53 phosphoresidues. These were probed by western blot analysis on p53 phosphorylated by CK1 α and δ at a concentration close to its K_m value (750 nM). As shown in Fig. 5b, p53 immunoreacts with specific antibodies raised against phospho-S9, phospho-S15, phospho-S20, and phospho-S37, but not with the phospho-S6, phospho-T18, phospho-S46, and phospho-S392 antibodies. Lack of immunoreaction with phospho-p53 (T18) antibody

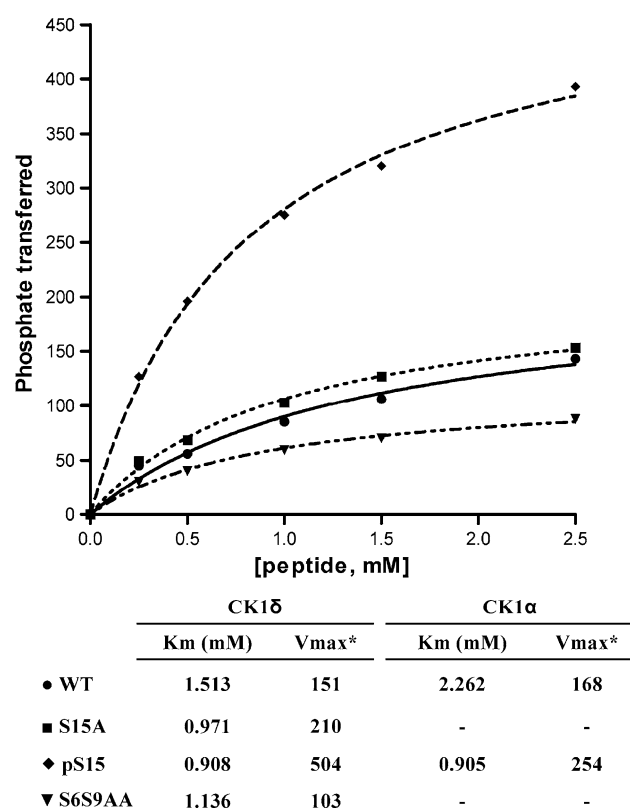


Fig. 4 Kinetics of p53 peptides phosphorylation by CK1 α and δ . The indicated peptides were subjected to phosphorylation with CK1 α (not shown on graph) and δ as described in “Materials and methods”. Initial rate data were fitted to the Michaelis–Menten equation to obtain V_{\max} and K_m values reported in the *inset*. * V_{\max} is expressed as picomoles of phosphate transferred per minute per unit of enzyme (one unit being defined as the amount of enzyme that transfers 1 nmol of phosphate per minute on the I–2 reference peptide). Therefore, they are not representative of specific activity. See “Materials and methods” for details

reinforces the view that T18 phosphorylation is a primed event detectable only if previous substantial phosphorylation of S15 by protein kinases other than CK1 takes place. Although the data shown in Fig. 5 were obtained using GST-p53 as phosphorylatable substrate, no significant differences could be observed if this was replaced by untagged p53 (see caption of Fig. 5).

In an attempt to evaluate differences in phosphorylation efficiency among the p53 sites affected by CK1 δ kinetics were performed in which the phosphorylation of individual residues was detected and quantified by western blotting with the phosphospecific antibodies. The experimental curves are shown in Fig. 6 and the calculated K_m values, which are independent of the sensitivity of the different antibodies, are reported in the inset. It appears that the highest affinity (K_m value even lower than that of the p53 protein as a whole) is displayed by S20, followed by S9 (with twofold higher K_m), while the K_m values of S15 and S37 are 10- and >20-fold higher than that of S20,

respectively. In the inset of Fig. 6, the V_{\max} values are also reported; it should be warned, however, that these are not suitable for a comparative analysis since they were calculated from data with different antibodies, whose sensitivity can be quite variable. Also of interesting in the case of full-size p53 (as already observed with the peptide) the phosphorylation of S20 is critically dependent on E17 whose replacement with alanine in the E17A mutant causes a dramatic drop in S20 phosphorylation (Fig. 5c).

Taken collectively, these data are consistent with a phosphorylation pattern of full-length p53 by CK1 δ similar to that observed with the peptide, with a marked preference for S20, as compared to S9, not to say S15 and S37 (this latter not included in the peptide anyway), whose K_m for CK1 δ is one order of magnitude higher. S6 despite its consensus sequence is not significantly phosphorylated either in the peptide (Fig. 3a) or in the protein (Fig. 5b). Likewise, non-primed phosphorylation of T18 by CK1 could not be detected in full-size p53, consistent with the view that its phosphorylation needs to be primed by stoichiometric amounts of phospho-S15 which cannot be generated under our conditions.

Thus, the only remarkable difference between full-length p53 and the peptide is the much lower affinity of the latter, strongly suggesting that a remote docking site is present in p53 which ensures high affinity binding to CK1 δ and α isoforms. In an attempt to identify such a putative docking site, we have concentrated our attention on a region which is conserved in the δ , ϵ , and α isoforms of CK1 but not in the γ isoforms. A sequence fulfilling such criteria is the K²²¹RQK²²⁴ quartet belonging to the loop next to the G helix in CK1 δ (see Fig. 7a). Indeed, the analysis of the possible interactions between CK1 δ and p53 through our protein–protein docking strategy suggests, for this quartet, one particular binding pose (see Fig. 7b). According to this model, the basic side chains of K221 and R222 interact with two acidic residues of p53, E224 and E228, respectively; note that these residues of p53 contribute to the most negatively charged stretch of the protein, where three acidic residues are clustered together (E221, E224, and E228). K224 of CK1 δ is not involved in this kind of interaction because of its implication in a tungstate ion bridge which connects the loop to the kinase core [2]. From the analysis of CK1 δ and γ sequences and crystal structures from the protein data bank, it is possible to note that the conserved K224 (an arginine in the γ isoforms) maintains its interactions with ions or water molecules in the same position. By sharp contrast, the substitution of K221 with a leucine residue in all γ isoforms is responsible for an alteration of the loop secondary structure, with an extension of the adjacent α -helix G. In this situation, the CK1 γ lysine residue, corresponding to CK1 δ R222, is moved back by about 4.7 Å, breaking the

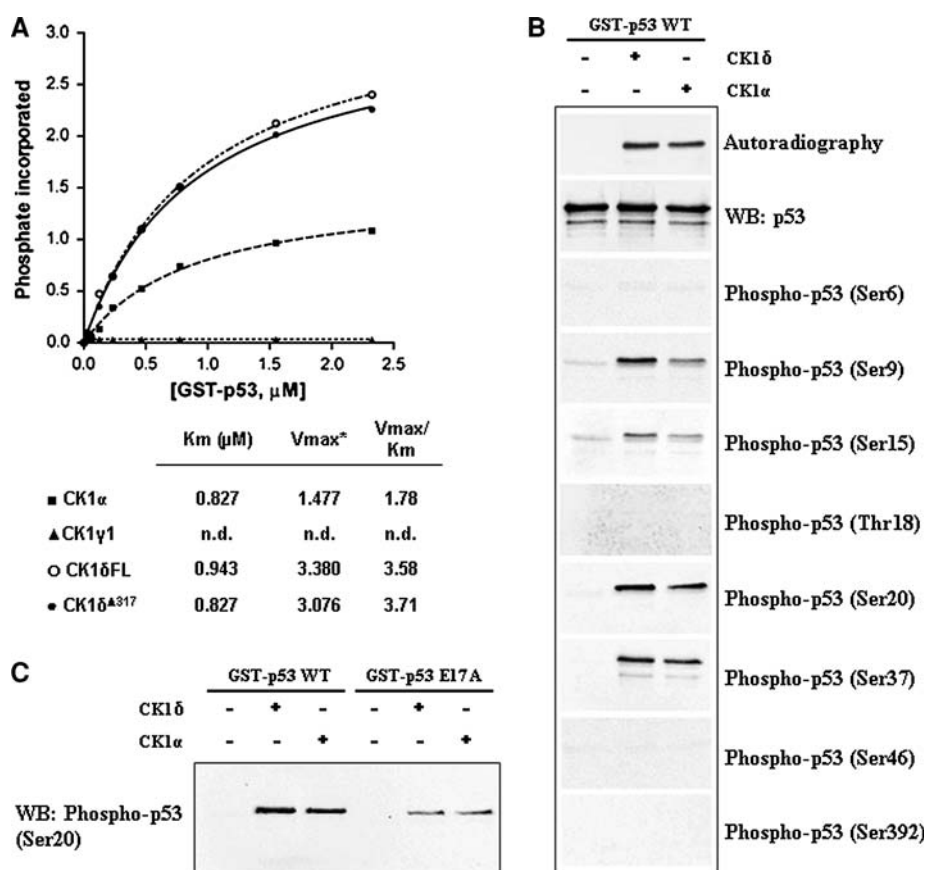


Fig. 5 Phosphorylation of p53 proteins by CK1 isoforms. **a** The kinetics of phosphorylation by CK1 isoforms of increasing concentrations of full-length GST-p53 wild-type are illustrated. p53 was subjected to phosphorylation with the indicated CK1 isoforms as described in “Materials and methods”. Of note are the identical kinetics of full-length and truncated ($\Delta 317$) CK1 δ , this latter sharing 95% identity with the ε isoform. V_{max} is expressed as picomoles of phosphate transferred per minute per unit of enzyme; *n.d.* not determined due to undetectable phosphorylation. **b** Full-length human GST-p53 (1.2 μg) produced in *E. coli* was phosphorylated by 10 min incubation with either CK1 δ or α isoforms and subjected to western

immunoblotting analysis with the antibodies indicated on the right. Superimposable kinetics and phosphorylation pattern were obtained replacing GST-p53 with untagged p53 obtained by proteolytically removing of the tag (see “Materials and methods”). **c** Effect of the Glu17 to Ala mutation on p53 S20 phosphorylation by CK1. Equal amounts (1.2 μg) of full-length p53, either wild-type or E17A mutant, were incubated under the same conditions (see “Materials and methods”) with CK1 δ or CK1 α . Western immunoblot with the specific phospho-p53 (Ser20) antibody is shown. Densitometric analysis of the anti-phospho-S20 signal shows a remarkable decrease in phosphorylation of the E17A mutant by CK1 α (70%) and δ (90%)

interaction with p53 E228. Consequently, in the case of all CK1 γ isoforms, both the interactions with p53 E224 and E228 are missing, which may account for weaker affinity of CK1 γ_1 for p53, as compared to the α , δ , and ε isoforms.

This model has been validated by mutational data showing that replacement of K221 with leucine in CK1 δ has a detrimental effect on its ability to phosphorylate p53 (Fig. 7c). In contrast, the mutation of K224 which, according to the model is not implicated in the interactions with p53, has no appreciable effect on p53 phosphorylation.

Discussion

Plenty of data in the literature support the implication of CK1 in the regulation of the tumour suppressor gene

product p53, as amply documented in all recent reviews listing CK1 among the numerous kinases participating in the complicated mechanism of p53 modulation [42–44]. However, the identification of the CK1 isoforms implicated, as well as of the individual p53 residues affected, and of the mechanism underlying their targeting by CK1, is still poorly understood. In tables and cartoons summarizing p53 multi-phosphorylation, CK1 (with special reference to its δ and ε isoforms, nearly identical with each other) is invariably represented as an “N-terminal” p53 kinase impinging on S6 and S9, the latter presumably through a hierarchical mechanism, after S6 has been phosphorylated. Of note is that S6 displays the consensus for unprimed phosphorylation by CK1 owing to two acidic residues at positions n-3 and n-4 (E-E-p-q-S⁶). Its phosphorylation by CK1, however, is not supported by incontrovertible

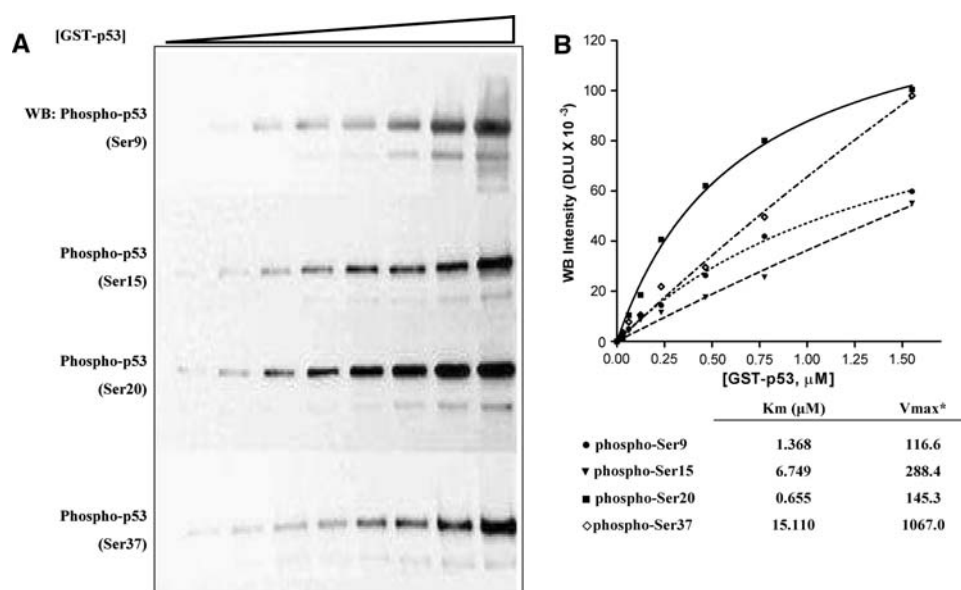


Fig. 6 Kinetic analysis of individual phosphoacceptor residues upon phosphorylation of full length p53 by CK1 δ . **a** The effect due to increasing concentration of p53 on the phosphorylation rate of S9, S15, S20, and S37 was monitored by western blotting with specific phospho-serine antibodies. **b** The specific phospho-serine bands detected in (**a**) were quantified by densitometric analysis using the Kodak 1D image analysis software and normalized to total p53

amount. Data were plotted against GST-p53 concentration using the Graphpad Prism software to calculate K_m and V_{max} values. V_{max} evaluated with the phospho-p53 (S15) antibody may represent an overestimate, since the intensity of this band unlike those of the other bands was not linear with incubation time, as it already reached a maximum intensity after 5 min. * V_{max} is expressed as densitometry light units (DLU)

evidence, while it has been reported to be a target for another kinase, JNK2 [65]. On the other hand, primed phosphorylation of T18 by CK1 isoforms has been independently reported by two groups as relying on previous phosphorylation of S15 [48, 49]. This latter appears to be a target for many kinases, notably DNA-PK, ATM, ATR, ERK, and p38 [50–53], but not for CK1. Recently, a work aimed at the identification of kinase(s) responsible for the phosphorylation of p53 at S20 in response to HHV-6B viral infection has led to the isolation of CK1 as the most likely cellular virus-induced S20 kinase [54]. Although S20 displays the minimum consensus for unprimed phosphorylation by CK1 (E-t-f-S²⁰), its phosphorylation was previously ascribed to kinases other than CK1, namely CHK1, CHK2 [55, 56], JNK, and MAPKAPK2 [57].

The results of our mechanistic study—the first systematically performed with different isoforms of CK1 tested on full-length p53 and on a set of variably substituted N-terminal p53 segments—strongly corroborates the concept that indeed S20 displays the features for being the preferred target for the δ and ϵ and, to a lesser extent, for the α isoforms of CK1 in unprimed p53, either full length or its N-terminal peptide. S20 is in fact the only seryl residue whose replacement with alanine in the peptide alone causes a >80% drop in phosphorylation rate (see Fig. 3), and whose phosphorylation in full-size p53 occurs

with a K_m in the sub-micromolar range, comparable to that displayed by p53 as such (see Figs. 5a and 6b).

Unlike the δ and α isoforms of CK1, CK1 γ_1 proved unable to catalyze any appreciable phosphorylation of p53 or of the p53 unprimed peptide. In contrast, primed phosphorylation of T18, specified by previous phosphorylation of S15, is readily performed by all the three isoforms of CK1, albeit with variable efficiencies (see Fig. 3).

Phosphorylation of S20 in the p53 peptide clearly relies on the minimum consensus generated by E17, since the substitution of this residue with alanine has a detrimental effect comparable to that of substituting S20 itself (see Fig. 3a). Interestingly, although a similar (and even “stronger”) consensus is present upstream from S6, this residue does not appear to be susceptible to phosphorylation by CK1, either in the peptide, where its substitution has no significant effect, or in full size p53 where its phosphorylation was flatly undetectable (Fig. 5b). Incidentally, this sheds doubt on the commonly held concept that phospho-S6 is required to prime S9 phosphorylation by CK1; it is quite clear from our experiments with recombinant GST-p53 that S9 is robustly phosphorylated by CK1 δ (Figs. 5b and 6) in the absence of any appreciable phosphorylation of S6. Additionally data with phosphopeptides show that the priming efficacy of phospho-S6 on S9 phosphorylation is not as pronounced as that of

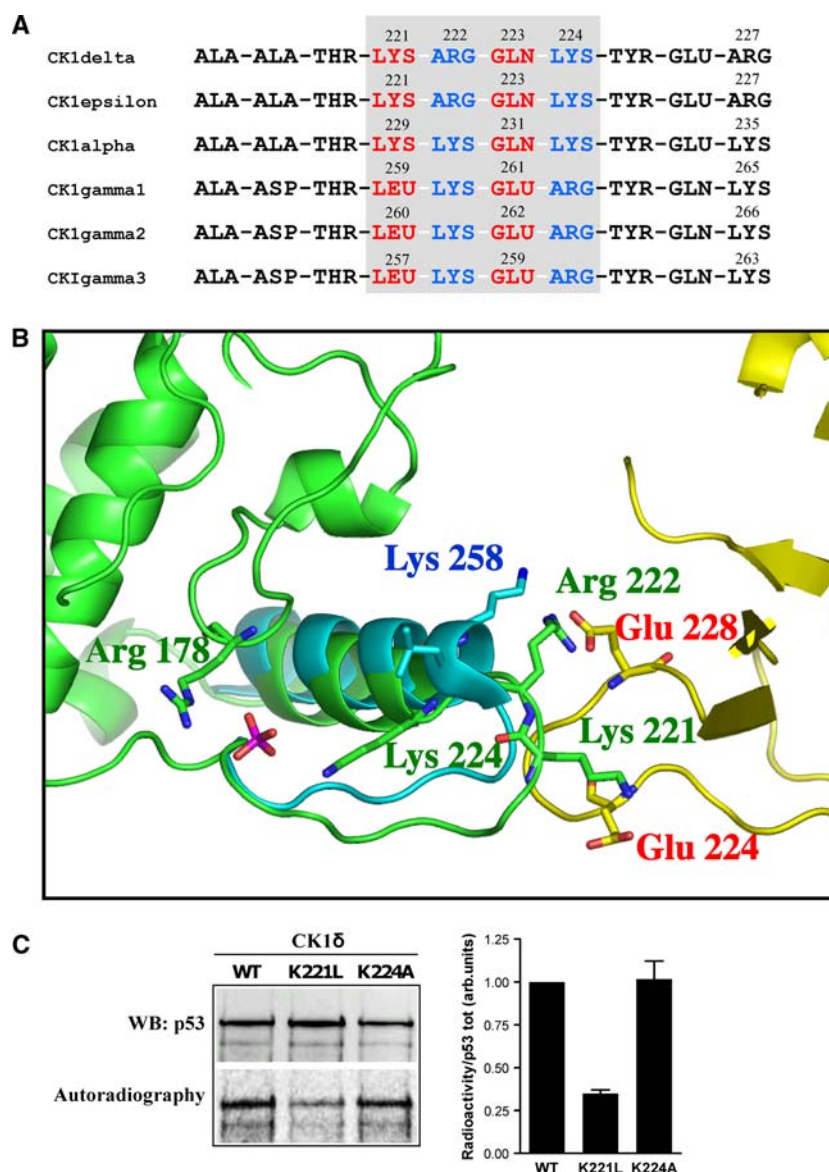


Fig. 7 Mapping the putative CK1 δ docking site responsible for high affinity binding of p53. **a** Multiple alignment of the α -helix G region in different CK1 isoforms. The four residues located in the basic loop adjacent to α -helix G are displayed in the gray box. This quartet is conserved between the δ/ϵ and α isoforms (with conservative substitution of R222 with lysine) while it is deeply altered in the γ isoforms. Mutation within the loop are in red, conserved basic residues are in blue. **b** Computer-aided protein–protein docking analysis of interaction motifs between CK1 δ isoform (green) and p53 (yellow). CK1 γ (blue) is unable to bind p53 due to the substitution of K221 with leucine which causes an extension of α -helix G, thus breaking the interaction between K258 (R222 in CK1 δ) and p53

E228. For additional explanation, see text. **c** Lys221 to Leu mutation drastically reduces the ability of CK1 δ to phosphorylate p53. GST-p53 was incubated for 10 min with equi-active amounts of either CK1 δ wild-type, or its K221L or K224A mutants under the conditions for protein phosphorylation, as detailed in “Materials and methods”. Western immunoblot with p53 antibody and autoradiography are shown. Densitometric analysis of western blot and of autoradiography was performed with Kodak 1D and with Optiquant (PerkinElmer) image analysis software, respectively. The results are also shown as a bar graph where p53 radioactivity has been normalized to total p53 amount

phospho-S15 on T18, which is not to say that it is entirely lacking with the γ isoform (see Fig. 3).

Somewhat unexpected was the finding that p53 undergoes significant phosphorylation by CK1 δ at S15, albeit with a K_m value denoting an affinity tenfold below that of S20 (K_m 6.74 vs 0.65 μ M; see Fig. 6b). The actual

intensity of S15 phosphorylation within full-size p53 may be also questionable considering that time course analysis with phospho-p53 (S15) antibody does not display time dependency as in the case of the other phosphosites (data not shown), suggesting that they might at least partially reflect an artefact due to the antibody. As a matter of fact,

S15 phosphorylation is not taking place within the peptide as judged from the observation that the individual substitution of S15 with alanine has no detrimental effect whatsoever (Fig. 3a).

It should be underscored in this respect, however, that high affinity targeting of full size p53 is critically relying on remote docking site(s) which are lost in the peptide, whose phosphorylation pattern therefore could incompletely reflect that of the full-size protein. This is unambiguously demonstrated by strikingly different kinetic constants calculated for CK1 δ and α phosphorylation of either the peptide or the protein at the same residues (with the marginal exception of S37). Although in fact the phosphorylation rate with the peptide is higher (V_{\max} 151 vs. 3.07 pmol per minute per unit of enzyme), its affinity is >3 orders of magnitude lower (K_m 1.51 mM as compared to 0.82 μ M), consistent with the view that physiological targeting of p53 by CK1 requires high affinity interactions between a remote complementary domain, which is lost in passing from full-size p53 to its N-terminal segment. A similar situation has been described in the case of p53 serine 20 phosphorylation after HHV-6B viral infection, whose occurrence depends on interaction of CK1 with Box IV and Box V domains of p53 [54]. It is likely that these elements are also responsible for the high affinity phosphorylation of full-size p53 as compared to its N-terminal peptide reported here. Our additional observation that such a phosphorylation is catalyzed by the α and δ/ϵ , but not by the γ , isoforms of CK1 would map the complementary docking site to a region which is not conserved in the γ isoforms. From the alignment of the CK1 isoforms, it appears that such a putative docking site might correspond to the K²²¹RQK²²⁴ sequence set on the loop next to the G-helix in CK1 δ . This basic sequence is conserved both in α (KKQK) and in ϵ (KRQK) isoforms but is lacking in all the γ isoforms where the first lysine is replaced by leucine and glutamine by glutamic acid (see Fig. 7a). The role of this motif as a remote docking site responsible for high affinity binding of p53 has been corroborated by computer-aided protein-protein docking strategy highlighting the special relevance of K221 which in the γ isoforms is replaced by a leucine. Such a model has been further validated by mutational analysis showing that replacement of K221 with leucine drastically impairs phosphorylation efficiency.

Interestingly, however, as in the case of β -catenin S45 phosphorylation by CK1 [41], phosphorylation of p53 S20 appears to depend not only on remote but also on local recognizing elements since replacement of E17 with alanine is equally detrimental in the N-terminal peptide and in full-size p53 despite the ability of this latter to interact with the remote docking site present in both CK1 δ and CK1 α (see Fig. 5c).

References

- Knippschild U, Gocht A, Wolff S, Huber N, Löhler J, Stöter M (2005) The casein kinase 1 family: participation in multiple cellular processes in eukaryotes. *Cell Signal* 17(6):675–689
- Longenecker KL, Roach PJ, Hurley TD (1996) Three-dimensional structure of mammalian casein kinase I: molecular basis for phosphate recognition. *J Mol Biol* 257:618–631
- Xu RM, Carmel G, Sweet RM, Kuret J, Cheng X (1995) Crystal structure of casein kinase-1, a phosphate-directed protein kinase. *EMBO J* 14:1015–1023
- Brockman JL, Gross SD, Sussman MR, Anderson RA (1992) Cell cycle-dependent localization of casein kinase I to mitotic spindles. *Proc Natl Acad Sci USA* 89:9454–9458
- Milne DM, Looby P, Meek DW (2001) Catalytic activity of protein kinase CK1 delta (casein kinase 1 delta) is essential for its normal subcellular localization. *Exp Cell Res* 263:43–54
- Petronczki M, Matos J, Mori S, Gregan J, Bogdanova A, Schwickart M, Mechtler K, Shirahige K, Zachariae W, Nasmyth K (2006) Monopolar attachment of sister kinetochores at meiosis I requires casein kinase 1. *Cell* 126:1049–1064
- Behrend L, Milne DM, Stoter M, Deppert W, Campbell LE, Meek DW, Knippschild U (2000) IC261, a specific inhibitor of the protein kinases casein kinase 1-delta and -epsilon, triggers the mitotic checkpoint and induces p53-dependent postmitotic effects. *Oncogene* 19:5303–5313
- Behrend L, Stoter M, Kurth M, Rutter G, Heukeshoven J, Deppert W, Knippschild U (2000) Interaction of casein kinase 1 delta (CK1delta) with post-Golgi structures, microtubules and the spindle apparatus. *Eur J Cell Biol* 79:240–251
- Camacho F, Cilio M, Guo Y, Virshup DM, Patel K, Khorkova O, Styren S, Morse B, Yao Z, Keesler GA (2001) Human casein kinase I delta phosphorylation of human circadian clock proteins period 1 and 2. *FEBS Lett* 489:159–165
- Zhu J, Shibasaki F, Price R, Guillemot JC, Yano T, Dotsch V, Wagner G, Ferrara P, McKeon F (1998) Intramolecular masking of nuclear import signal on NF-AT4 by casein kinase I and MEKK1. *Cell* 93:851–861
- Peters JM, McKay RM, McKay JP, Graff JM (1999) Casein kinase I transduces Wnt signals. *Nature* 401:345–350
- Zeng X, Tamai K, Doble B, Li S, Huang H, Habas R, Okamura H, Woodgett J, He X (2005) A dual-kinase mechanism for Wnt co-receptor phosphorylation and activation. *Nature* 438:873–877
- Davidson G, Wu W, Shen J, Bilic J, Fenger U, Stanek P, Glinka A, Niehrs C (2005) Casein kinase 1 gamma couples Wnt receptor activation to cytoplasmic signal transduction. *Nature* 438:867–872
- Hämmerlein A, Weiske J, Huber O (2005) A second protein kinase CK1-mediated step negatively regulates Wnt signalling by disrupting the lymphocyte enhancer factor-1/beta-catenin complex. *Cell Mol Life Sci* 62(5):606–618
- Swiatek W, Kang H, Garcia BA, Shabanowitz J, Coombs GS, Hunt DF, Virshup DM (2006) Negative regulation of LRP6 function by casein kinase I epsilon phosphorylation. *J Biol Chem* 281:12233–12241
- Price MA (2006) CKI, there's more than one: casein kinase I family members in Wnt and Hedgehog signaling. *Genes Dev* 20(4):399–410
- Bryja V, Schulte G, Rawal N, Grahn A, Arenas E (2007) Wnt-5a induces Dishevelled phosphorylation and dopaminergic differentiation via a CK1-dependent mechanism. *J Cell Sci* 120(4):586–595
- Beyaert R, Vanhaesebroeck B, Declercq W, Van Lint J, Vandenabeele P, Agostinis P, Vandenheede JR, Fiers W (1995) Casein kinase-1 phosphorylates the p75 tumor necrosis factor receptor

- and negatively regulates tumor necrosis factor signaling for apoptosis. *J Biol Chem* 270:23293–23299
19. Desagher S, Osen-Sand A, Montessuit S, Magnenat E, Vilbois F, Hochmann A, Journot L, Antonsson B, Martinou JC (2001) Phosphorylation of bid by casein kinases I and II regulates its cleavage by caspase 8. *Mol Cell* 8:601–611
 20. Schwab C, DeMaggio AJ, Ghoshal N, Binder LI, Kuret J, McGeer PL (2000) Casein kinase 1 delta is associated with pathological accumulation of tau in several neurodegenerative diseases. *Neurobiol Aging* 21:503–510
 21. Yasojima K, Kuret J, DeMaggio AJ, McGeer E, McGeer PL (2000) Casein kinase 1 delta mRNA is upregulated in Alzheimer disease brain. *Brain Res* 865:116–120
 22. Xu Y, Padiath QS, Shapiro RE, Jones CR, Wu SC, Saigoh N, Saigoh K, Ptacek LJ, Fu YH (2005) Functional consequences of a CKI delta mutation causing familial advanced sleep phase syndrome. *Nature* 434:640–644
 23. Elias L, Li AP, Longmire J (1981) Cyclic adenosine 3':5'-monophosphate-dependent and -independent protein kinase in acute myeloblastic leukemia. *Cancer Res* 41:2182–2188
 24. Mishra SK, Yang Z, Mazumdar A, Talukder AH, Larose L, Kumar R (2004) Metastatic tumor antigen 1 short form (MTA1 s) associates with casein kinase I-gamma2, an estrogen-responsive kinase. *Oncogene* 23:4422–4429
 25. Frierson HF Jr, El-Naggar AK, Welsh JB, Sapinoso LM, Su AI, Cheng J, Saku T, Moskaluk CA, Hampton GM (2002) Large scale molecular analysis identifies genes with altered expression in salivary adenoid cystic carcinoma. *Am J Pathol* 161:1315–1323
 26. Fuja TJ, Lin F, Osann KE, Bryant PJ (2004) Somatic mutations and altered expression of the candidate tumor suppressors CSNK1 epsilon, DLG1, and EDD/hHYD in mammary ductal carcinoma. *Cancer Res* 64:942–951
 27. Adorno M, Cordenonsi M, Montagner M, Dupont S, Wong C, Hann B, Solari A, Bobisse S, Rondina MB, Guzzardo V, Parenti AR, Rosato A, Biciato S, Balmain A, Piccolo S (2009) A Mutant-p53/Smad complex opposes p63 to empower TGFbeta-induced metastasis. *Cell* 137:87–98
 28. Meggio F, Donella-Deana A, Pinna LA (1979) Studies on the structural requirements of a microsomal cAMP-independent protein kinase. *FEBS Lett* 106(1):76–80
 29. Flotow H, Graves PR, Wang AQ, Fiorello CJ, Roeske RW, Roach PJ (1990) Phosphate groups as substrate determinants for casein kinase I action. *J Biol Chem* 265(24):14264–14269
 30. Meggio F, Perich JW, Reynolds EC, Pinna LA (1991) A synthetic beta-casein phosphopeptide and analogues as model substrates for casein kinase-1, a ubiquitous, phosphate directed protein kinase. *FEBS Lett* 283(2):303–306
 31. Roach PJ (1991) Multisite and hierarchical protein phosphorylation. *J Biol Chem* 266(22):14139–14142
 32. Amit S, Hatzubai A, Birman Y, Andersen JS, Ben-Shushan E, Mann M, Ben-Neriah Y, Alkalay I (2002) Axin mediated CKI phosphorylation of β -catenin at Ser 45: a molecular switch for the Wnt pathway. *Genes Dev* 16:1066–1076
 33. Liu C, Li Y, Semenov M, Han C, Baeg GH, Tan Y, Zhang Z, Lin X, He X (2002) Control of β -catenin phosphorylation/degradation by a dual-kinase mechanism. *Cell* 108:837–847
 34. Ha NC, Tonzuka T, Stamos JL, Choi HJ, Weis WI (2004) Mechanism of phosphorylation-dependent binding of APC to β -catenin and its role in β -catenin degradation. *Mol Cell* 15:511–521
 35. Xing Y, Clements WK, Le Trong I, Hinds TR, Stenkamp R, Kimelman D, Xu W (2004) Crystal structure of a β -catenin/APC complex reveals a critical role for APC phosphorylation in APC function. *Mol Cell* 15:523–533
 36. Ferrarese A, Marin O, Bustos VH, Venerando A, Antonelli M, Allende JE, Pinna LA (2007) Chemical dissection of the APC Repeat 3 multistep phosphorylation by the concerted action of protein kinases CK1 and GSK3. *Biochemistry* 46(42):11902–11910
 37. Desdouits F, Siciliano JC, Greengard P, Girault JA (1995) Dopamine- and cAMP-regulated phosphoprotein DARPP-32: phosphorylation of Ser-137 by casein kinase I inhibits dephosphorylation of Thr-34 by calcineurin. *Proc Natl Acad Sci USA* 92(7):2682–2685
 38. Pulgar V, Marin O, Meggio F, Allende CC, Allende JE, Pinna LA (1999) Optimal sequences for non-phosphate-directed phosphorylation by protein kinase CK1 (casein kinase-1)—a re-evaluation. *Eur J Biochem* 260(2):520–526
 39. Marin O, Burzio V, Boschetti M, Meggio F, Allende CC, Allende JE, Pinna LA (2002) Structural features underlying the multisite phosphorylation of the A domain of the NF-AT4 transcription factor by protein kinase CK1. *Biochemistry* 41(2):618–627
 40. Marin O, Bustos VH, Cesaro L, Meggio F, Pagano MA, Antonelli M, Allende CC, Pinna LA, Allende JE (2003) A noncanonical sequence phosphorylated by casein kinase I in beta-catenin may play a role in casein kinase I targeting of important signaling proteins. *Proc Natl Acad Sci USA* 100(18):10193–10200
 41. Bustos VH, Ferrarese A, Venerando A, Marin O, Allende JE, Pinna LA (2006) The first armadillo repeat is involved in the recognition and regulation of beta-catenin phosphorylation by protein kinase CK1. *Proc Natl Acad Sci USA* 103(52):19725–19730
 42. Bode AM, Dong Z (2004) Post-translational modification of p53 in tumorigenesis. *Nat Rev Cancer* 4:793–805
 43. Lacroix M, Toillon RA, Leclercq G (2006) p53 and breast cancer, an update. *Endocr Relat Cancer* 13(2):293–325
 44. Appella E, Anderson CW (2001) Post-translational modifications and activation of p53 by genotoxic stresses. *Eur J Biochem* 268(10):2764–2772
 45. Knippschild U, Milne DM, Campbell LE, DeMaggio AJ, Christenson E, Hoekstra MF, Meek DW (1997) p53 is phosphorylated in vitro and in vivo by the delta and epsilon isoforms of casein kinase I and enhances the level of casein kinase I delta in response to topoisomerase-directed drugs. *Oncogene* 15(14):1727–1736
 46. Higashimoto Y, Saito S, Tong XH, Hong A, Sakaguchi K, Appella E, Anderson CW (2000) Human p53 is phosphorylated on serines 6 and 9 in response to DNA damage-inducing agents. *J Biol Chem* 275(30):23199–23203
 47. Cordenonsi M, Montagner M, Adorno M, Zacchigna L, Martello G, Mamidi A, Soligo S, Dupont S, Piccolo S (2007) Integration of TGF-beta and Ras/MAPK signaling through p53 phosphorylation. *Science* 315(5813):840–843
 48. Dumaz N, Milne DM, Meek DW (1999) Protein kinase CK1 is a p53-threonine 18 kinase which requires prior phosphorylation of serine 15. *FEBS Lett* 463(3):312–316
 49. Sakaguchi K, Saito S, Higashimoto Y, Roy S, Anderson CW, Appella E (2000) Damage-mediated phosphorylation of human p53 threonine 18 through a cascade mediated by a casein I-like kinase. Effect on Mdm2 binding. *J Biol Chem* 275(13):9278–9283
 50. Shieh SY, Ikeda M, Taya Y, Prives C (1997) DNA damage induced phosphorylation of p53 alleviates inhibition by MDM2. *Cell* 91:325–334
 51. Saito S, Goodarzi AA, Higashimoto Y, Noda Y, Lees-Miller SP, Appella E, Anderson CW (2002) ATM mediates phosphorylation at multiple p53 sites, including Ser(46), in response to ionizing radiation. *J Biol Chem* 277:12491–12494
 52. Tibbetts RS, Brumbaugh KM, Williams JM, Sarkaria JN, Cliby WA, Shieh SY, Taya Y, Prives C, Abraham RT (1999) A role for ATR in the DNA damage-induced phosphorylation of p53. *Genes Dev* 13:152–157

53. She QB, Chen N, Dong Z (2000) ERKs and p38 kinase phosphorylate p53 protein at serine 15 in response to UV radiation. *J Biol Chem* 275:20444–20449
54. MacLaine NJ, Oster B, Bundgaard B, Fraser JA, Buckner C, Lazo PA, Meek DW, Höllsberg P, Hupp TR (2008) A central role for CK1 in catalyzing phosphorylation of the p53 transactivation domain at serine 20 after HHV-6B viral infection. *J Biol Chem* 283(42):28563–28573
55. Chehab NH, Malikzay A, Stavridi ES, Halazonetis TD (1999) Phosphorylation of Ser-20 mediates stabilization of human p53 in response to DNA damage. *Proc Natl Acad Sci USA* 96:13777–13782
56. Unger T, Juven-Gershon T, Moallem E, Berger M, Vogt Sionov R, Lozano G, Oren M, Haupt Y (1999) Critical role for Ser20 of human p53 in the negative regulation of p53 by Mdm2. *EMBO J* 18:1805–1814
57. She QB, Ma WY, Dong Z (2002) Role of MAP kinases in UVB-induced phosphorylation of p53 at serine 20. *Oncogene* 21:1580–1589
58. Fields GB, Noble RL (1990) Solid phase peptide synthesis utilizing 9-fluorenylmethoxycarbonyl amino acids. *Int J Pept Protein Res* 35:161–214
59. Burzio V, Antonelli M, Allende CC, Allende JE (2002) Biochemical and cellular characteristics of the four splice variants of protein kinase CK1 α from zebrafish (*Danio rerio*). *J Cell Biochem* 86:805–814
60. Marin O, Meggio F, Pinna LA (1994) Design and synthesis of two new peptide substrates for the specific and sensitive monitoring of casein kinases-1 and -2. *Biochem Biophys Res Commun* 198:898–905
61. Perich JW, Meggio F, Reynolds EC, Marin O, Pinna LA (1992) Role of phosphorylated aminoacyl residues in generating atypical consensus sequences which are recognized by casein kinase-2 but not by casein kinase-1. *Biochemistry* 31:5893–5897
62. Molecular operating environment (MOE 2008.10), C.C.G., Inc., 1255 University St., Suite 1600, Montreal, Quebec, Canada H3B 3X3
63. Cozza G, Moro S, Gotte G (2008) Elucidation of the ribonuclease A aggregation process mediated by 3D domain swapping: a computational approach reveals possible new multimeric structures. *Biopolymers* 89:26–39
64. Poletto G, Vilardell J, Marin O, Pagano MA, Cozza G, Sarno S, Falqués A, Itarte E, Pinna LA, Meggio F (2008) The regulatory beta subunit of protein kinase CK2 contributes to the recognition of the substrate consensus sequence. A study with an eIF2 beta-derived peptide. *Biochemistry* 47:8317–8325
65. Oleinik NV, Krupenko NI, Krupenko SA (2007) Cooperation between JNK1 and JNK2 in activation of p53 apoptotic pathway. *Oncogene* 26:7222–7230